
FlowSpec: Continuous Pipelined Speculative Decoding for Efficient Distributed LLM Inference

Xing Liu^{1*}Lizhuo Luo^{2*}Ming Tang¹Chao Huang³

Abstract

Distributed inference serves as a promising approach to enabling the inference of large language models (LLMs) at the network edge. It distributes the inference process to multiple devices to ensure that the LLMs can fit into the device memory. Recent pipeline-based approaches have the potential to parallelize communication and computation, which helps reduce inference latency. However, the benefit diminishes when the inference request at the network edge is sparse, where pipeline is typically at low utilization. To enable efficient distributed LLM inference at the edge, we propose **FlowSpec**, a pipeline-parallel tree-based speculative decoding framework. FlowSpec incorporates three key mechanisms to improve decoding efficiency: 1) score-based step-wise verification prioritizes more important draft tokens to bring earlier accepted tokens; 2) efficient draft management to prune invalid tokens while maintaining correct causal relationship during verification; 3) dynamic draft expansion strategies to supply high-quality speculative inputs. These techniques work in concert to enhance both pipeline utilization and speculative efficiency. We evaluate FlowSpec on a real-world testbed with other baselines. Experimental results demonstrate that our proposed framework significantly improves inference speed across diverse models and configurations, achieving speedup ratios $1.36\times$ - $1.77\times$ compared to baselines. Our code is publicly available at <https://github.com/Leosang-lx/FlowSpec#>

1 Introduction

Large language models (LLMs) have been widely adopted in intelligent applications in various domains such as education, finance, and Internet of Things (IoT). However, due to their massive size, LLM inference is commonly performed at the cloud, which can introduce significant response delay due to the long-distance transmission between users and centralized servers. Moreover, cloud-based inference often requires uploading sensitive user data, raising concerns of privacy leakage.

As a result, deploying LLM inference at the network edge has emerged a promising approach to mitigate transmission overhead and enhance data privacy [Gill et al., 2025], particularly beneficial for industrial IoT and smart homes [Chang et al., 2021]. However, there are two main challenges. First, edge devices such as smartphones or embedded systems typically have limited memory (several GB), making it difficult to run advanced LLMs like LLaMA2 [Touvron et al., 2023a] or Qwen2 [Yang et al., 2024] with tens of billions of parameters (e.g., a 7B model requires over 14GB memory in FP16 precision). Second, their computational capabilities of edge devices are often restricted to CPUs or low-memory GPUs, causing high inference latency. While model compression techniques like pruning [Sanh et al., 2020] and quantization [Lin et al., 2024, Xiao et al., 2023] have been explored, they often incur performance degradation. A promising alternative is *distribute inference* [Ye et al.,

*Equal contribution ¹Department of Computer Science and Engineering, Southern University of Science and Technology ²Department of Statistics and Data Science, Southern University of Science and Technology ³School of Computing, Montclair State University. Corresponding author: tangm3@sustech.edu.cn

2024, Zhang et al., 2024], which partitions an LLM across multiple devices to enable collaborative and parallel inference, overcoming memory constraints and reduce inference latency.

One widely adopted approach in distributed inference is pipeline parallelism (PP) [Huang et al., 2019, Zhang et al., 2024], which partitions a model into stages and assigns them to different devices. The pipeline then processes multiple inputs sequentially in a pipelined fashion, overlapping computation with communication and achieving more efficient communication compared to other parallel strategies¹. However, *the effectiveness of PP diminishes with sparse inference requests*, which commonly occurs in LLM inference at the edge. Specifically, the generation of each token relies on the previous one, traditional autoregressive decoding cannot be parallelized across the pipeline stages. Therefore, sparse inference requests lead to insufficient parallelism across different stages of the pipeline, resulting in frequent pipeline cold starts (i.e., the period for the first input to pass through all pipeline stages) and hardware under-utilization. In addition, naive autoregressive LLM decoding is inherently I/O-bound [Leviathan et al., 2023] due to the low-FLOPs forward propagation and frequent access to KV cache. This issue is exacerbated in distributed scenarios, which can lead to additional communication overhead.

To address this, speculative decoding (SD) [Leviathan et al., 2023] was proposed to accelerate LLM decoding. SD generates multiple draft tokens using a lightweight draft model and verifies them in parallel through the base LLM to ensure a correct inference output, enabling the generation of multiple tokens in a single forward pass. This alleviates the decoding I/O-bound under sparse-request scenario. However, traditional SD typically relies on synchronous draft generation and verification, which limits the efficiency of SD. In particular, the autoregressive draft generation on the draft model remains a bottleneck in SD, especially on resource-constrained edge devices where computation capacity and I/O bandwidth are both limited.

To this end, researchers have investigated distributed speculative LLM decoding under pipelined architectures with asynchronous drafting and verification [Butler et al., 2024, Yin et al., 2025] to accelerate single-request LLM inference. By deploying the draft model and the base LLM on different devices, the current verification on the base LLM can be paralleled with the generation of new draft tokens on the draft model, achieving continuous SD on pipeline and thus reducing the cold starts overheads. However, designing a continuous speculative decoding on pipeline system is non-trivial. On the one hand, the tree-structure draft tokens should be managed carefully and efficiently, the invalid draft tokens should be discarded in real time while ensuring correct causal relationship between the remaining tokens. On the other hand, the asynchronous draft generation should maintain a continuous supply of high-quality draft for the pipeline to ensure a good continuity of speculative decoding in pipeline.

In this work, we propose a pipeline-parallel tree-based speculative decoding framework for distributed LLM inference in edge environments. It extends tree-based SD into pipeline-based distributed inference system, enabling parallel inference among multiple devices to fully explore resource utilization potentials and reduce inference latency. Different from existing works, FlowSpec prioritizes high-scoring draft tokens through scores-based tree segmentation, and continuously feeds the pipeline with high-quality draft tokens based on the latest context, significantly improves the throughput of single-request decoding with pipeline parallelism. In addition, we propose tree pruning and expansion techniques to enable *continuous verification* by the base LLM, which reduces resource waste and avoids frequent cold starts. Our key contributions are summarized as follows:

- FlowSpec adopts score-aware step-wise verification of the draft tree across the pipeline system. By evaluating draft tokens based on their confidence scores from the draft model, FlowSpec prioritizes high-probability draft tokens, enabling earlier token acceptance and accelerating speculative decoding.
- FlowSpec introduces a fine-grained draft management mechanism to minimize redundant overhead in SD. It enables efficient collaborative pruning of invalid tokens and their KV cache across distributed devices, preserving causal relationships while maintaining memory efficiency. The system also proactively exits verification when all draft are invalid, avoiding unnecessary computation.

¹Other approaches include tensor parallelism (TP) [Shoeybi et al., 2019] and sequence parallelism (SP) [Li et al., 2021], while this paper focuses on PP. Please refer to Appendix B for detailed discussions.

- FlowSpec employs novel draft tree expansion strategies to sustain a steady supply of new draft tokens and improve the continuity of pipelined SD. Instead of simply expanding the current tree from the bottom, FlowSpec generates a new draft tree when the context is updated and merges it with the existing one, otherwise extends the current tree by selecting high-score nodes from the extended candidate drafts.
- To evaluate FlowSpec, we deploy it on a real-world testbed and compare its performance with state-of-the-art baselines under various settings, including different base models and datasets. Experimental results show that FlowSpec achieves $1.35\times$ – $1.73\times$ speedups in decoding compared to naive pipeline, demonstrating its effectiveness in improving inference performance.

2 Related Works

Distributed LLM Inference on Edge: Previous works proposed optimized TP-based approaches to mitigate its communication overhead in edge scenarios. For example, DeTransformer [Wei et al., 2024] reduces the number of communications in TP by modifying the model structure. Voltage [Hu and Li, 2024] reduces communication overhead in TP by reordering general matrix multiplications (GEMMs) and replacing All-Reduce with All-Gather. GALAXY [Ye et al., 2024] combines TP and SP for fine-grained computation-communication overlap. However, these TP-based approaches require intra-layer communications for data synchronization in each decoder layer, leading to large communication and synchronization latency under the low-bandwidth connections between edges. Other studies proposed to deploy pipeline parallelism (PP) to enable collaborative LLM inference. SARATHI [Agrawal et al., 2023] proposes to split the input sequence into chunks and feeding them into the pipeline progressively, enabling parallel processing during the LLM prefilling phase to enhance performance. EdgeShard [Zhang et al., 2024] deploys LLMs at the edge using PP, reducing overhead through load balancing and improving system throughput by optimizing pipeline bubbles. *However, these approaches may incur a large inference latency in sparse-request scenarios.*

Speculative Decoding: Speculative decoding (SD) [Leviathan et al., 2023] was proposed to accelerate LLM inference. Build upon this framework, many works focus on tree-based SD to improve token acceptance. For example, SpecInfer [Miao et al., 2024] and Medusa [Cai et al., 2024] generate multiple candidate tokens at each step, organizing them into a tree structure to enable parallel verification. Some works proposed leveraging contextual information to improve the quality of draft tokens by context-aware SD. EAGLE [Li et al., 2024a] predicts feature sequences of draft tokens by leveraging the hidden states from the base model as input and applies tree-based decoding in the construction of the draft token tree. GLIDE and CAPE [Du et al., 2024] utilize the KV cache of the base model to predict draft tokens and dynamically adjust the number of draft tokens based on confidence scores. Besides, EAGLE-2 [Li et al., 2024b] and OPT-Tree [Wang et al., 2025] dynamically construct draft trees based on accumulated confidence scores from the draft model, enabling context-aware and adaptive tree structures that improve both efficiency and generation accuracy. *However, the above works focused on centralized inference scenarios, which cannot be directly applied to distributed inference at network edge.*

Distributed SD: Recent works proposed to extend SD into distributed inference system to address the sparse-request scenario. For example, Jupiter [Ye et al., 2025] partitions input sequences during prefilling and enables task-level parallel SD, while it applies to only specific outline-based tasks. AMUSD [McDanel, 2024] performs asynchronous drafting and verification on a two-stage pipeline, yet only supports sequence drafting. PipeInfer [Butler et al., 2024] fills pipeline bubbles with normal decoding and draft verification, but its simple generation of multiple draft trees introduces significant redundancy across stages. Additionally, its complicated draft management degrades system efficiency. Although recent work PipeDec [Yin et al., 2025] considered pruning and expansion of draft tree to implement continuous SD in pipeline. However, its layer-by-layer draft tree verification significantly limits the decoding throughput, and expanding the tree only from the bottom also restricts the continuity of context-aware SD approaches in pipeline.

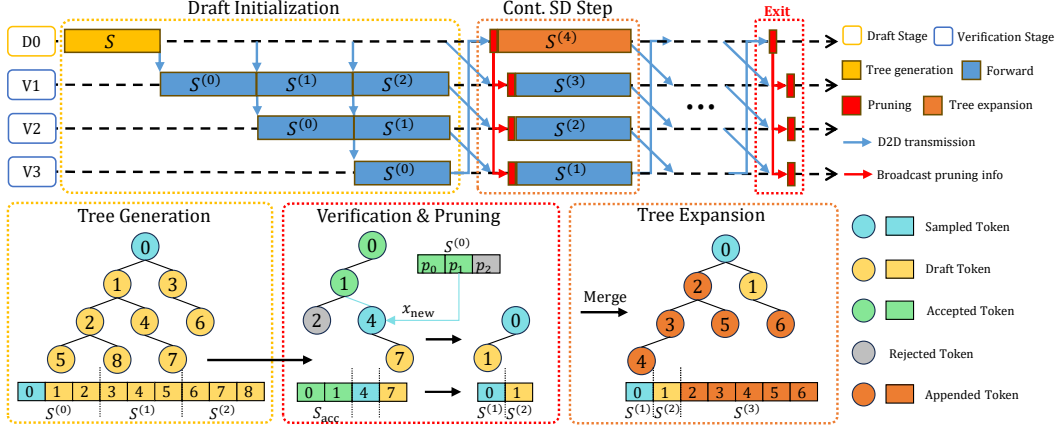


Figure 1: Overview of FlowSpec: An SD round includes a draft initialization step and multiple continuous SD steps. In draft initialization, segments of the initial generated draft tree are fed to V1 to fill all pipeline stages. Once the first subsequence completes all inference stages, the subsequent continuous SD steps begin. In each step, the current tree is pruned based on the accepted tokens, and then expanded to generate new draft tokens that serve as input for the next step.

3 Methodology

3.1 FlowSpec Overview

We propose a pipeline-parallel tree-based speculative decoding framework for distributed inference, called FlowSpec. It divides the layers of the base LLM into different pipeline stages. Motivated by evaluating draft tokens based on the output scores of the draft model from EAGLE-2 [Li et al., 2024b], FlowSpec incorporates a score-based draft tree step-wise verification framework with dynamic pruning and expansion strategies tailored for continuous speculative decoding in pipeline systems. Moreover, our framework can be generalized to other state-of-the-art tree-based SD approaches.

Consider $N + 1$ devices in our system, each device corresponds to a pipeline stage. The first stage (device 0) employing the draft model is called the **draft stage** (denoted by "D0"), which is responsible for draft generation and accepting valid tokens based on the verification outputs from the base LLM. The base LLM is partitioned into N consecutive layers blocks distributed to the rest N devices, with device n serving as the n -th **verification stage** (denoted by " Vn "). These stages are responsible for executing the corresponding forward pass during the verification of draft tokens in the base LLM. In Figure 1, the upper part shows devices 0 to $N = 3$ and their associated draft state D0 and verification stages V1 to V3.

To serve an LLM inference request, the input prompt is first processed in the **prefilling phase**. It is fed into the verification stages (i.e., forward pass from V1 to VN) to compute the initial KV cache and generate the first sampled token x_{new} through the base LLM. To accelerate the prefilling phase for long input sequence, we adopt chunked prefill [Agrawal et al., 2023], i.e., splitting the input prompt into segments and processing them sequentially across pipeline.

After prefilling, the system starts the **decoding phase** (see Figure 1), which is the main focus of FlowSpec, including the score-based step-wise draft verification, together with efficient tree pruning and expansion design in real time. This phase consists of multiple SD **rounds**, each round contains an draft initialization step and a set of continuous SD steps:

1) Draft Initialization Step: D0 first generates a large draft token tree \mathcal{T}_{base} based on the latest sampled token x_{new} , and selects the top-scoring nodes to form a refined draft tree \mathcal{T} for subsequent verification. Then, the associated draft sequence S (descending order of scores) of \mathcal{T} is divided into $N + 1$ segments $S^{(0)}, \dots, S^{(N)}$, each with a length no greater than L_{max} . This length is determined by hardware constraints. The draft segments $S^{(0)}, \dots, S^{(N)}$ are then sequentially fed into the pipeline of the verification stages (i.e., from V1 to VN). For example, in Figure 1, D0 first sends $S^{(0)}$ to V1. Upon the completion of $S^{(0)}$ on V1, the intermediate result of $S^{(0)}$ is sent to V2 and then to V3. Once the first draft segment $S^{(0)}$ completes all verification stages and D0 receives the first verification

output of $S^{(0)}$, the continuous SD step starts. Note that the other segments are continuously being verified in the pipeline. For example, after $S^{(0)}$ completes VN, $S^{(1)}$ enters VN for execution.

2) Continuous SD Steps: Once a draft segment $S^{(i)}$ completes all verification stages V1 to VN, its verification output (i.e., the next-token distribution from the base LLM) is sent to D0 for evaluation. With the verification result, D0 determines the accepted prefix and a new sampled token (i.e., x_{new} updates). The continuous SD steps of the current round continue and all other draft segments proceed to the next verification stage if the latest x_{new} satisfies the **continuous condition** (detailed in 3.3). Otherwise, the current round terminates and a new round is initiated.

In each continuous SD step, D0 executes the following two operations:

- **Tree Pruning:** If D0 obtains a non-empty accepted prefix in the current continuous SD step, the current tree \mathcal{T} is pruned, retaining only the valid branches rooted at x_{new} . This process results in a smaller tree \mathcal{T}_{pr} . Note that all stages need to perform pruning over its local replicas of \mathcal{T} to discard invalid draft tokens.
- **Tree Expansion:** At each continuous SD step, D0 extends the current draft tree in two possible ways depending on whether new tokens are accepted. If new accepted tokens exist, D0 generate a new tree \mathcal{T}_{new} based on the updated context and merges it with \mathcal{T}_{pr} to form the updated \mathcal{T} . Otherwise, D0 continues the expansion of \mathcal{T} based on extended $\mathcal{T}_{\text{base}}$. The newly generated draft portion then serves as the input for V1 in the next step.

In the following discussion, unless specified, a draft sequence or segment implicitly includes its associated tree position IDs and tree attention mask.

3.2 Draft Initialization: Score-Based Step-Wise Draft Verification

In draft initialization step, D0 first constructs a draft token tree \mathcal{T} of depth d_0 with L nodes in the draft stage D0. Note that each node in the tree corresponds to a token in LLM inference, so we use "node" and "token" interchangeable in the following. The root of this tree is the sampled token x_{new} generated either in the prefilling phase or the previous rounds of SD. The construction of token tree contains the following procedures.

Initial Tree Generation: D0 sets the root node (layer 0) to be the latest x_{new} . Then, it uses the draft model to generate the initial tree $\mathcal{T}_{\text{base}}$. The tree is initially rooted at x_{new} and extended layer by layer based on the nodes with the highest cumulative scores (inspired by Eagle-2 [Li et al., 2024b]) in each layer. The cumulative score for node n_i in a draft token tree is defined as follows:

$$c_{\text{cu}}(n_i) = \prod_{n_j \in \text{path}(n_i)} c(n_j) = c_{n_i} \times c_{\text{cu}}(\text{parent}(n_j)), \quad (1)$$

where $\text{path}(n_i)$ denotes all ancestor nodes along the path from the root node to n_i . Since the draft model is an approximation of the base LLM, this cumulative score provides a nice estimated acceptance score of a draft token. To construct the next layer of $\mathcal{T}_{\text{base}}$, the draft model takes the tokens from the previous layer as input and generates the corresponding next-token scores. Base on these scores, the top- k next tokens for each input token form the new layer of $\mathcal{T}_{\text{base}}$. Among these, the top- k nodes with the highest cumulative scores are selected to continue the expansion of the next layer. D0 expands $\mathcal{T}_{\text{base}}$ until it reaches layer d_0 .

Score-Based Draft Segmentation: Then the top- L nodes in $\mathcal{T}_{\text{base}}$ with the highest cumulative scores are selected to obtain the refined draft token tree \mathcal{T} , with the corresponding draft token sequence S sorted in descending order of the draft token scores. Since a node always has a higher cumulative score than its children, the selected nodes can form a connected tree \mathcal{T} . Then S is split into consecutive, equal-length draft segments $S^{(0)}, \dots, S^{(N)}$ with maximum length of l_{max} . These segments are then fed into the verification pipeline one after the other.

Sorting the nodes based on their cumulative score have two advantages. First, since the cumulative score of a node is an estimate of its importance, the descending-score order prioritizes the verification of higher-scoring draft tokens, increasing the likelihood accepting more tokens in advance, thereby enabling faster and deeper expansion of the draft token tree. Second, since a parent node always has a higher score than its children, this ordering of the draft segments establishes a valid topological order of the tree \mathcal{T} , which ensures correct causal relationship between tokens in the subsequent step-wise verification (i.e., a preceding token must be ahead of its successors in verification).

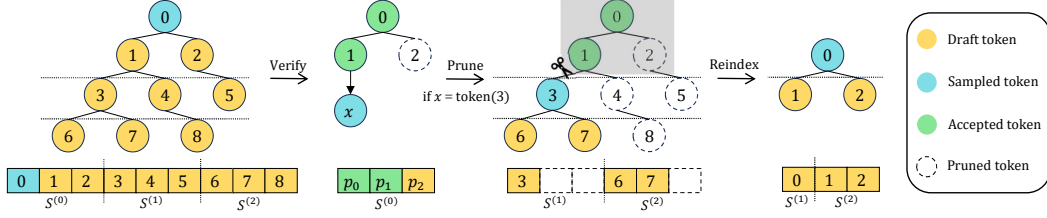


Figure 2: An example of tree pruning showing by the indices of the draft tokens. The above part is of the tree form, and the below is the sequence. In this case, $\mathcal{I}_{acc} = \{0, 1\}$ and $\mathcal{I}_{draft} = \{3, 6, 7\}$.

3.3 Continuous SD: Tree Pruning

In each continuous SD step, once a draft segment $S^{(i)}$ completes all verification stages, D0 receives the corresponding final hidden state of the base LLM, and computes the output probability of $S^{(i)}$. By comparing the output distributions from the draft model and the base model, tokens that leads to an aligned distribution are accepted, denoted by S_{acc} . Meanwhile, an additional sampled token x_{new} is generated based on the output probability and S_{acc} . After that, D0 determines whether to continue the current SD round according to the **continuous condition**. The continuous condition is defined as:

$$\text{continuous_condition} := \exists n_{new} \in \mathcal{T} \text{ s.t. } \text{path}_{\mathcal{T}}(n_{new}) = \{S_{acc} || x_{new}\}, \quad (2)$$

where " $||$ " denotes sequence concatenation. If x_{new} satisfies the continuous condition, which means x_{new} is already in the verification pipeline corresponding to the node $n_{new} \in \mathcal{T}$, thus the current SD round continues. **Otherwise, all remaining draft tokens become invalid**, therefore FlowSpec exits the current SD round and initiate a new one.

The tree pruning process is illustrated in Figure 2. To prune \mathcal{T} , D0 identifies all invalid branches according to S_{acc} and x_{new} . The nodes to retain include n_{new} and all its descendant nodes in \mathcal{T} , and these nodes form the pruned tree \mathcal{T}_{pr} with root node n_{new} . The corresponding pruned sequence S_{pr} preserves the original order of the retaining tokens in the origin sequence S .

Besides D0, V1 to VN also need consistent pruning to update their local draft segments. Let \mathcal{I}_{acc} and \mathcal{I}_{pr} denote the ordered sets of indices of the accepted tokens and retaining tokens of \mathcal{T}_{pr} in the sequence S before pruning, respectively. D0 sends the full retaining set $\mathcal{I}_{retain} = \mathcal{I}_{acc} \cup \mathcal{I}_{pr}$ as the pruning information to all downstream stages V1 to VN. Let l_{glo} denote the global context offset (i.e., the total number of tokens of the full input prompt and all accepted tokens), which will be updated by $l_{glo} = l_{glo} + |S_{acc}|$ after each pruning procedure. Then each element in \mathcal{I}_{retain} is incremented by l_{glo} such that the element indicates the position index of the associated token in the global sequence. For each stage, the pruning operation is applied to both the local draft segment and KV cache based on the following two index sets:

- **Segment Pruning:** The local positions in the current draft segment corresponding to the tokens that need to be retained in the pruned tree \mathcal{T}_{pr} , defined as $\mathcal{I}_{local} = \{i - l_{cache} | i \in \mathcal{I}_{retain}, l_{cache} \leq i < l_{cache} + l_s\}$. Here, l_{cache} and l_s denote the length of the KV cache and the length of the draft segment at the current stage, respectively. The indices are mapped from the global positions to local draft segment positions by subtracting l_{cache} .
- **KV cache pruning:** The indices of nodes (tokens) to be retained in the KV cache are those associated with indices in set $\mathcal{I}_{in-cache} = \{i \in \mathcal{I}_{retain} | i < l_{cache}\}$. Since KV cache includes the complete context, the indices used for cache pruning correspond to global positions.

To prune a local draft segment (including the associated hidden states, tree position IDs and attention mask), we retain only the entries corresponding to \mathcal{I}_{local} , and the full draft sequence S is accordingly pruned to be S_{pr} . To prune the KV cache, we first retain the KV cache entries corresponding to the previous context (i.e., positions before l_{glo}). For the KV cache associated with the draft tokens (i.e., positions $\geq l_{glo}$), we only keep the entries whose indices match $\mathcal{I}_{in-cache}$. This enables each stage to remove redundant KV cache entries and intermediate data related to pruned tokens, ensuring both consistency and memory efficiency in subsequent decoding steps.

In this way, FlowSpec efficiently performs collaborative pruning on the irregular draft segments across the distributed pipeline system with low communication overhead, while maintaining correct causal relationship between all tokens throughout the entire lifecycle of the growing draft token tree.

3.4 Continuous SD: Tree Expansion

Unless the current SD round terminates, D0 performs tree expansion at the end of each continuous SD step. This process expands the current draft token tree to sustain continuous supply of new draft tokens for verification and hence reduces the chance of cold starts in pipeline parallelism. There are two possible situations for tree expansion as follows:

Context-aware Expansion. D0 performs context-aware expansion immediately after finishing the pruning operation. As the existing draft tokens in \mathcal{T}_{pr} are generated based on stale context, they have limited reliability for SD under the updated context. In contrast, new draft tokens incorporate more up-to-date contextual information, making them more accurate and reliable. Therefore, instead of expanding the pruned tree from the bottom, FlowSpec grows a new tree from the current root node and merge them together, effectively improving the continuity for SD on pipeline.

In addition to the pruned tree \mathcal{T}_{pr} rooted with x_{new} , D0 generates a new tree \mathcal{T}_{new} based on the newly accepted S_{acc} and sampled x_{new} , with size L_{exp} and d_{exp} from the root node x_{new} . The generation of \mathcal{T}_{new} is of the same manner as generating the initial \mathcal{T} in draft initialization step (\mathcal{T}_{base} is also updated with a new one, and \mathcal{T}_{new} is a subtree of \mathcal{T}_{base}). Then, \mathcal{T}_{pr} and \mathcal{T}_{new} are merged as \mathcal{T}_{mer} as the update to \mathcal{T} . Specifically, the nodes in \mathcal{T}_{new} that are new to \mathcal{T}_{pr} are selected and appended to \mathcal{T}_{pr} as \mathcal{T}_{mer} . We determine whether a node in \mathcal{T}_{new} is a new draft token

by checking if the path corresponding to the node exists in \mathcal{T}_{pr} . D0 preloads the path set of \mathcal{T}_{pr} as $\mathcal{P}_{pr} = \{\text{path}_{\mathcal{T}_{pr}}(n) | n \in \mathcal{T}_{pr}\}$, utilizing a hash table to efficiently store and distinguish nodes corresponding to different paths. Then the set of new draft tokens can be expressed by $\mathcal{N}_{new} = \{n \in \mathcal{T}_{new} | \text{path}_{\mathcal{T}_{new}}(n) \notin \mathcal{P}_{pr}\}$. To get the expanded draft sequence corresponding to \mathcal{T}_{mer} , the new draft tokens are appended to the end of the existing complete draft sequence S_{pr} as $S_{mer} = \{S_{pr} || S_{app}\}$. Here S_{app} is the draft sequence of \mathcal{N}_{new} , which will serve as the new draft input for verification pipeline. An illustration is shown in Fig. 3. This process guarantees that the draft tokens already in the pipeline retain their original sequential order and appear at the front of the merged draft sequence, ensuring accurate causal structure between the current set of draft tokens.

Score-aware Expansion. Since pruning operations are applied to the remaining draft segments, some segments received by the D0 may already be reduced to empty sequence. In this case, the context is not updated, further propagating the empty sequence can cause continuous idle pipeline. To ensure a continuous supply of new draft tokens, D0 also expands \mathcal{T} at this point. Specifically, D0 first expands the initial tree \mathcal{T}_{base} (which is preserved for tree expansion). Starting from the deepest layer, \mathcal{T}_{base} is extended by additional d_{se} layers (as mentioned in 3.2), forming a deeper tree \mathcal{T}'_0 . From this extended \mathcal{T}'_0 , we exclude all nodes already exists in the current tree \mathcal{T} , and select the top- L_{se} nodes with the highest cumulative scores among the remaining ones. These nodes are then appended to the current tree \mathcal{T} , similar to the appending tokens in tree merging. Their corresponding draft sequence S_{se} are then fed into pipeline as the new supplied draft tokens. The current draft sequence is also updated with $S \leftarrow \{S || S_{se}\}$. In this way, we effectively verifies a larger draft tree, leading to a higher acceptance rate of draft tokens while ensuring a steady stream of new drafts for pipelined verification.

4 Experiment

4.1 Setups

Hardware. The experiments were conducted on 5 NVIDIA Jetson Orin Nano units, each equipped with 8GB of RAM, interconnected via a local area network.

Models and Datasets. We evaluated the performance of FlowSpec on 4 models within the EAGLE-2 framework, i.e., LLaMA-Chat 7B, 13B [Touvron et al., 2023b] and Vicuna-v1.3 7B, 13B [Chiang

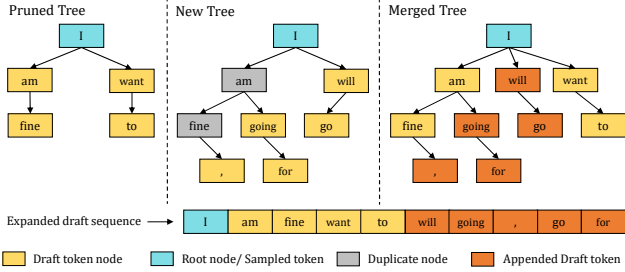


Figure 3: An example explaining merging the old pruned draft tree and the newly generated draft tree.

et al., 2023]. The weights of the draft models and base models are sourced from `huggingface.co`. The method’s performance is validated across 6 downstream tasks, i.e., multi-turn dialogue, code generation, mathematical reasoning, instruction understanding, text summarization, and question answering. The associated datasets are MT-bench [Zheng et al., 2023], HumanEval [Chen et al., 2021], GSM8K [Cobbe et al., 2021], Alpaca [Taori et al., 2023], CNN/Daily Mail [Nallapati et al., 2016], and Natural Questions [Kwiatkowski et al., 2019], respectively.

Baselines. We compare FlowSpec against 2 representative baselines, i.e., *Naive Pipeline Parallelism (Naive PP)* and *PipeDec*. Naive PP partitions the speculative decoding model distributed across multiple devices, enabling the input data to be processed in a pipelined fashion. PipeDec [Yin et al., 2025] is a state-of-the-art method for distributed speculative decoding model that employs pipeline parallelism in resource constrained environment. We will show in the following that FlowSpec significantly outperforms the baselines in both inference efficiency and resource utilization.

Metrics. We consider the following metrics:

- **Average Acceptance Length per Second ξ :** The average number of tokens generated per second, which reflects the overall operational efficiency of the inference system.
- **Speedup Ratio (SR):** The inference acceleration achieved compared to the baselines.

To ensure accurate time measurements, each method undergoes the same warm-up procedure prior to testing in order to equalize cache hit rates.

Implementation Details. We build a testbed using NVIDIA JetPack 5.1.2 (L4T R35.4.1) with CUDA 11.4 support. We employ the ARM-aarch64-specific PyTorch 1.11.0+cu114 [Paszke et al., 2019], installed via NVIDIA’s official Python 3.8 wheel. Our core codebase extends the original EAGLE-2 implementation. To deploy the 13B parameter model on the rest 4 NVIDIA Jetson Orin Nano units, we employed W4A16 quantization (4-bit storage while preserving 16-bit computation precision) via the `bitsandbytes` library integrated in Hugging Face `transformers`. **More Detailed experimental settings are provided in the Appendix.**

4.2 Main Results

Table 1 presents the results of FlowSpec and the baselines across multiple tasks on 4 LLM models. From the table, we observe that FlowSpec significantly outperforms both Naive PP and PipeDec on a variety of tasks. Across multiple tasks, FlowSpec achieves an average speedup of up to **1.73×** compared to Naive PP.

Temperature = 0. Under the greedy sampling strategy, FlowSpec’s average performance on each model surpasses that of PipeDec and Naive PP. Specifically, on the Vicuna-v1.3 13B model, it achieves a 1.70× speedup over Naive PP, whereas PipeDec only attains a 1.49× speedup under the same conditions. More specifically, FlowSpec achieves a 1.76× speedup on the instruction understanding (Alpaca) dataset with the Vicuna-v1.3 13B model, demonstrating the effectiveness of our method. It is evident that FlowSpec delivers nearly consistent speedups across different tasks. For example, on the LLaMA2-Chat 13B model it achieves an approximately 1.67× speedup, demonstrating that our method is effective and exhibits both robustness and stability under a variety of conditions. Overall, FlowSpec illustrates effectiveness and robustness at temperature = 0.

Temperature = 1. Table 1 highlights FlowSpec’s remarkable advantage: on the Vicuna-v1.3 13B model, it runs 1.73× faster than Naive PP at temperature = 1. Under the same settings, it delivers a 1.86× boost on the code generation task (HumanEval). Moreover, it generates 7.65 tokens/s on the LLaMA2-Chat 7B on average, demonstrating outstanding efficacy. Owing to the uncertainty inherent in stochastic sampling, the acceleration achieved across different datasets and models exhibits appreciable variability. FlowSpec consistently delivers significant speedups across a variety of models and tasks.

Under the Vicuna-v1.3 7B model as the base model with temperature=1, FlowSpec’s performance is marginally inferior to that of PipeDec. This is mainly due to the high decoding stochasticity and low draft acceptance rates from the draft model, leading to frequent cold starts in both approaches. Compared to FlowSpec, PipeDec’s layer-wise expansion strategy incurs slightly lower cold-start overhead, which may contribute to its modest performance gain in such cases. Nevertheless, FlowSpec still demonstrates overall superiority and efficiency.

Table 1: **Main Results**, which contain the performance comparison between FlowSpec and the baselines across 6 datasets under two sampling settings (Temperature = 0 or 1, 0 means greedy sampling). We select 20 samples for each dataset and limit the length of the generated sequences to 128. V and L2 are short for LLaMA2-Chat and Vicuna-v1.3, respectively. 7B and 13B denote the number of parameters of the respective models.

Model	Method	MT-bench		HumanEval		GSM8K		Alpaca		CNN/DM		Natural Ques.		Mean	
		$\xi\uparrow$	SR \uparrow												
Temperature = 0															
V 13B	Naive PP	0.98	1.00 \times	1.23	1.00 \times	1.20	1.00 \times	1.06	1.00 \times	0.62	1.00 \times	0.81	1.00 \times	0.98	1.00 \times
	PipeDec	1.43	1.46 \times	1.54	1.25 \times	1.54	1.28 \times	1.48	1.40 \times	1.17	1.89\times	1.33	1.64 \times	1.42	1.49 \times
	FlowSpec	1.66	1.69\times	2.05	1.67\times	2.02	1.68\times	1.80	1.70\times	1.09	1.76 \times	1.45	1.74\times	1.67	1.70\times
V 7B	Naive PP	6.58	1.00 \times	5.29	1.00 \times	6.30	1.00 \times	5.95	1.00 \times	3.46	1.00 \times	4.07	1.00 \times	5.28	1.00 \times
	PipeDec	6.99	1.06 \times	6.71	1.27 \times	7.19	1.14 \times	6.95	1.17 \times	5.14	1.49\times	5.88	1.44\times	6.48	1.23 \times
	FlowSpec	8.93	1.36\times	7.55	1.43\times	8.60	1.37\times	8.28	1.39\times	4.74	1.37 \times	5.78	1.42 \times	7.31	1.38\times
L2 13B	Naive PP	1.40	1.00 \times	1.60	1.00 \times	1.35	1.00 \times	1.22	1.00 \times	1.09	1.00 \times	1.11	1.00 \times	1.30	1.00 \times
	PipeDec	1.62	1.16 \times	1.64	1.02 \times	1.60	1.19 \times	1.56	1.28 \times	1.43	1.31 \times	1.52	1.37 \times	1.56	1.20 \times
	FlowSpec	2.29	1.64\times	2.69	1.68\times	2.26	1.67\times	2.04	1.67\times	1.81	1.66\times	1.89	1.70\times	2.16	1.66\times
L2 7B	Naive PP	7.05	1.00 \times	7.56	1.00 \times	6.24	1.00 \times	6.13	1.00 \times	4.56	1.00 \times	5.28	1.00 \times	6.14	1.00 \times
	PipeDec	7.27	1.03 \times	7.36	0.97 \times	7.12	1.14 \times	7.08	1.15 \times	5.79	1.27 \times	6.67	1.26 \times	6.88	1.12 \times
	FlowSpec	9.43	1.34\times	10.07	1.33\times	8.71	1.40\times	8.28	1.35\times	6.10	1.34\times	7.33	1.39\times	8.32	1.35\times
Temperature = 1															
V 13B	Naive PP	0.79	1.00 \times	0.73	1.00 \times	0.81	1.00 \times	0.88	1.00 \times	0.70	1.00 \times	0.70	1.00 \times	0.77	1.00 \times
	PipeDec	1.37	1.73 \times	1.26	1.73 \times	1.40	1.73 \times	1.21	1.38 \times	1.34	1.91 \times	1.32	1.89 \times	1.32	1.71 \times
	FlowSpec	1.38	1.75\times	1.36	1.86\times	1.36	1.68\times	1.47	1.67\times	1.17	1.67\times	1.26	1.80\times	1.33	1.73\times
V 7B	Naive PP	4.12	1.00 \times	4.15	1.00 \times	3.71	1.00 \times	4.56	1.00 \times	3.13	1.00 \times	3.47	1.00 \times	3.86	1.00 \times
	PipeDec	6.19	1.50\times	6.34	1.53\times	5.92	1.60\times	6.28	1.38\times	5.12	1.64\times	5.64	1.63\times	5.92	1.53\times
	FlowSpec	5.76	1.40 \times	5.77	1.39 \times	5.47	1.47 \times	6.17	1.35 \times	4.63	1.48 \times	5.16	1.49 \times	5.49	1.42 \times
L2 13B	Naive PP	1.36	1.00 \times	1.51	1.00 \times	1.22	1.00 \times	1.20	1.00 \times	1.02	1.00 \times	1.15	1.00 \times	1.24	1.00 \times
	PipeDec	1.61	1.18 \times	1.66	1.10 \times	1.60	1.31 \times	1.55	1.29 \times	1.45	1.42 \times	1.55	1.35 \times	1.57	1.27 \times
	FlowSpec	2.18	1.60\times	2.29	1.52\times	2.09	1.71\times	1.99	1.66\times	1.67	1.64\times	1.82	1.58\times	2.01	1.62\times
L2 7B	Naive PP	6.46	1.00 \times	6.48	1.00 \times	5.95	1.00 \times	5.87	1.00 \times	4.17	1.00 \times	5.04	1.00 \times	5.66	1.00 \times
	PipeDec	7.11	1.10 \times	7.06	1.09 \times	7.25	1.22 \times	7.13	1.21 \times	5.78	1.39 \times	6.82	1.35 \times	6.86	1.21 \times
	FlowSpec	8.53	1.32\times	8.63	1.33\times	8.43	1.42\times	7.54	1.28\times	5.79	1.39\times	7.00	1.39\times	7.65	1.35\times

Table 2: **Ablation Results** using the LLaMA2-Chat 7B model, showing average acceptance length per second (ξ) and latency across four datasets under two sampling settings (Temperature = 0 or 1). We select 10 samples from each dataset.

Method	MT-bench		HumanEval		GSM8K		Alpaca		Mean		
	$\xi\uparrow$	Latency \downarrow	SR \uparrow								
Temperature = 0											
Naive PP	7.11	25.64	7.41	51.63	6.48	35.17	6.37	43.03	6.84	38.87	1.00 \times
Pruned PP	8.52	20.89	8.73	42.66	8.19	27.07	8.22	31.69	8.42	30.58	1.23 \times
FlowSpec w/o SBD	9.31	34.25	9.33	42.10	8.61	26.84	8.75	29.94	9.00	33.28	1.17 \times
FlowSpec	9.61	18.35	10.00	37.38	8.93	25.20	8.85	30.43	9.35	27.84	1.37\times
Temperature = 1											
Naive PP	6.95	28.00	6.72	59.94	6.37	39.70	6.15	42.82	6.55	42.62	1.00 \times
Pruned PP	8.17	21.51	7.94	51.08	7.84	27.75	7.64	33.96	7.90	33.58	1.21 \times
FlowSpec w/o SBD	9.06	18.59	8.67	45.20	8.39	26.95	7.86	28.59	8.50	29.83	1.30 \times
FlowSpec	9.10	19.53	9.15	38.87	8.64	25.85	8.01	35.27	8.73	29.88	1.33\times

4.3 Ablation Study

Table 2 presents the results for different module configurations of FlowSpec on multiple tasks using LLaMA2-Chat 7B under two sampling conditions (Temperature = 0 or 1). *Naive Pipeline Parallelism (Naive PP)* follow the same setting above. *Pruned Pipeline Parallelism (Pruned PP)* extends Naive PP by leveraging Tree Pruning on the speculative decoding tree structure and incorporating early-exit strategies. *FlowSpec w/o Score-Based Draft (FlowSpec w/o SBD)* refer to the variant that applies Tree Expansion on top of Pruned PP as well as omitting the Score-Based Draft Segmentation. The different combinations of components confirm the effectiveness of each module.

Score-Based Draft Segmentation. Comparing FlowSpec to FlowSpec w/o Score-Based Draft in Table 2 directly highlights the positive impact of the Score-Based component. By sorting draft tokens according to contextual scores, Score-Based Draft Segmentation increases the accepted rate within segments and enhances the quality of expansion drafts. As a result, FlowSpec achieves an average throughput of 8.49 tokens/s at temperature = 0 and 8.02 tokens/s at temperature = 1, both of which exceed the performance of the method without Score-Based Draft Segmentation.

Tree Pruning. The difference between Naive Pipeline Parallelism and Pruned Pipeline Parallelism highlights the effectiveness of tree pruning: enabling pruning yields a 1.25× speedup over Naive PP, demonstrating a clear performance improvement. Redundant computations in tree-based speculative decoding substantially degrade inference efficiency.

Tree Expansion. Although the effectiveness of Tree Expansion is largely contingent on the draft model’s quality, our experiments nonetheless demonstrate substantial speedups. Notably, on the multi-turn dialogue task, FlowSpec without Score-Based Draft achieves throughputs of 9.06 and 9.31 tokens per second at temperature settings of 0 and 1, respectively—far surpassing Pruned Pipeline Parallelism. This indicates that when the draft model is sufficiently capable, Tree Expansion delivers pronounced performance gains.

5 Conclusion

In this work, we proposed FlowSpec, a pipeline-parallel tree-based speculative decoding framework, which reduces the LLM inference latency in distributed system at network edge with sparse requests. To improve resource utilization and avoid cold starts of pipeline, we introduced three main techniques to achieve efficient continuous speculative decoding: (i) score-based step-wise verification to bring earlier accepted tokens in speculative decoding (ii) efficient draft management including tree pruning and early stop to eliminate redundant device computations. (iii) real-time tree expansion to ensure a continuous flow of high-quality draft tokens, maintaining decoding continuity. To evaluate the system performance, we constructed a testbed. Experimental results demonstrate the superiority of our method over the baseline.

References

- Amey Agrawal, Ashish Panwar, Jayashree Mohan, Nipun Kwatra, Bhargav S Gulavani, and Ramachandran Ramjee. Sarathi: Efficient llm inference by piggybacking decodes with chunked prefills. *arXiv preprint arXiv:2308.16369*, 2023.
- Branden Butler, Sixing Yu, Arya Mazaheri, and Ali Jannesari. Pipeinfer: Accelerating llm inference using asynchronous pipelined speculation. In *SC24: International Conference for High Performance Computing, Networking, Storage and Analysis*, pages 1–19, 2024. doi: 10.1109/SC41406.2024.00046.
- Tianle Cai, Yuhong Li, Zhengyang Geng, Hongwu Peng, Jason D. Lee, Deming Chen, and Tri Dao. Medusa: Simple llm inference acceleration framework with multiple decoding heads. In *Proceedings of the 41st International Conference on Machine Learning, ICMML’24*. JMLR.org, 2024.
- Zhuoqing Chang, Shubo Liu, Xingxing Xiong, Zhaohui Cai, and Guoqing Tu. A survey of recent advances in edge-computing-powered artificial intelligence of things. *IEEE Internet of Things Journal*, 8(18):13849–13875, 2021. doi: 10.1109/IJOT.2021.3088875.
- Mark Chen, Jerry Tworek, Heewoo Jun, Qiming Yuan, Henrique Pondé, Jared Kaplan, Harrison Edwards, Yura Burda, Nicholas Joseph, Greg Brockman, Alex Ray, Raul Puri, Gretchen Krueger, Michael Petrov, Heidy Khlaaf, Girish Sastry, Pamela Mishkin, Brooke Chan, Scott Gray, Nick Ryder, Mikhail Pavlov, Alethea Power, Lukasz Kaiser, Mo Bavarian, Clemens Winter, Philippe Tillet, Felipe Petroski Such, David W. Cummings, Matthias Plappert, Fotios Chantzis, Elizabeth Barnes, Ariel Herbert-Voss, William H. Guss, Alex Nichol, Igor Babuschkin, Suchir Balaji, Shantanu Jain, Andrew Carr, Jan Leike, Joshua Achiam, Vedant Misra, Evan Morikawa, Alec Radford, Matthew M. Knight, Miles Brundage, Mira Murati, Katie Mayer, Peter Welinder, Bob McGrew, Dario Amodei, Sam McCandlish, Ilya Sutskever, and Wojciech Zaremba. Evaluating large language models trained on code. *ArXiv*, abs/2107.03374, 2021. URL <https://api.semanticscholar.org/CorpusID:235755472>.
- Wei-Lin Chiang, Zhuohan Li, Zi Lin, Ying Sheng, Zhanghao Wu, Hao Zhang, Lianmin Zheng, Siyuan Zhuang, Yonghao Zhuang, Joseph E. Gonzalez, Ion Stoica, and Eric P. Xing. Vicuna: An open-source chatbot impressing gpt-4 with 90%* chatgpt quality, March 2023. URL <https://lmsys.org/blog/2023-03-30-vicuna/>.

- Karl Cobbe, Vineet Kosaraju, Mo Bavarian, Mark Chen, Heewoo Jun, Lukasz Kaiser, Matthias Plappert, Jerry Tworek, Jacob Hilton, Reiichiro Nakano, Christopher Hesse, and John Schulman. Training verifiers to solve math word problems. *ArXiv*, abs/2110.14168, 2021. URL <https://api.semanticscholar.org/CorpusID:239998651>.
- Cunxiao Du, Jing Jiang, Xu Yuanchen, Jiawei Wu, Sicheng Yu, Yongqi Li, Shenggui Li, Kai Xu, Liqiang Nie, Zhaopeng Tu, and Yang You. Glide with a cape: a low-hassle method to accelerate speculative decoding. In *Proceedings of the 41st International Conference on Machine Learning, ICML'24*. JMLR.org, 2024.
- Sukhpal Singh Gill, Muhammed Golec, Jianmin Hu, Minxian Xu, Junhui Du, Huaming Wu, Guneet Kaur Walia, Subramaniam Subramanian Murugesan, Babar Ali, Mohit Kumar, et al. Edge ai: A taxonomy, systematic review and future directions. *Cluster Computing*, 28(1):1–53, 2025.
- Chenghao Hu and Baochun Li. When the edge meets transformers: Distributed inference with transformer models. In *2024 IEEE 44th International Conference on Distributed Computing Systems (ICDCS)*, pages 82–92, 2024. doi: 10.1109/ICDCS60910.2024.00017.
- Yanping Huang, Youlong Cheng, Ankur Bapna, Orhan Firat, Dehao Chen, Mia Chen, HyoukJoong Lee, Jiquan Ngiam, Quoc V Le, Yonghui Wu, et al. Gpipe: Efficient training of giant neural networks using pipeline parallelism. *Advances in neural information processing systems*, 32, 2019.
- Tom Kwiatkowski, Jennimaria Palomaki, Olivia Redfield, Michael Collins, Ankur Parikh, Chris Alberti, Danielle Epstein, Illia Polosukhin, Matthew Kelcey, Jacob Devlin, Kenton Lee, Kristina N. Toutanova, Llion Jones, Ming-Wei Chang, Andrew Dai, Jakob Uszkoreit, Quoc Le, and Slav Petrov. Natural questions: a benchmark for question answering research. *Transactions of the Association of Computational Linguistics*, 2019.
- Yaniv Leviathan, Matan Kalman, and Yossi Matias. Fast inference from transformers via speculative decoding. In *International Conference on Machine Learning*, pages 19274–19286. PMLR, 2023.
- Shenggui Li, Fuzhao Xue, Chaitanya Baranwal, Yongbin Li, and Yang You. Sequence parallelism: Long sequence training from system perspective. *arXiv preprint arXiv:2105.13120*, 2021.
- Yuhui Li, Fangyun Wei, Chao Zhang, and Hongyang Zhang. EAGLE: Speculative sampling requires rethinking feature uncertainty. In *International Conference on Machine Learning*, 2024a.
- Yuhui Li, Fangyun Wei, Chao Zhang, and Hongyang Zhang. EAGLE-2: Faster inference of language models with dynamic draft trees. In *Empirical Methods in Natural Language Processing*, 2024b.
- Ji Lin, Jiaming Tang, Haotian Tang, Shang Yang, Wei-Ming Chen, Wei-Chen Wang, Guangxuan Xiao, Xingyu Dang, Chuang Gan, and Song Han. Awq: Activation-aware weight quantization for llm compression and acceleration. In *MLSys*, 2024.
- Bradley McDanel. Amusd: Asynchronous multi-device speculative decoding for llm acceleration. *arXiv preprint arXiv:2410.17375*, 2024.
- Xupeng Miao, Gabriele Oliaro, Zhihao Zhang, Xinhao Cheng, Zeyu Wang, Zhengxin Zhang, Rae Ying Yee Wong, Alan Zhu, Lijie Yang, Xiaoxiang Shi, Chunan Shi, Zhuoming Chen, Daiyaan Arfeen, Reyna Abhyankar, and Zhihao Jia. Specinfer: Accelerating large language model serving with tree-based speculative inference and verification. In *Proceedings of the 29th ACM International Conference on Architectural Support for Programming Languages and Operating Systems, Volume 3, ASPLOS '24*, page 932–949, New York, NY, USA, 2024. Association for Computing Machinery. ISBN 9798400703867.
- Ramesh Nallapati, Bowen Zhou, Cícero Nogueira dos Santos, Çağlar Gülçehre, and Bing Xiang. Abstractive text summarization using sequence-to-sequence rnns and beyond. In *Conference on Computational Natural Language Learning*, 2016. URL <https://api.semanticscholar.org/CorpusID:8928715>.

- Adam Paszke, Sam Gross, Francisco Massa, Adam Lerer, James Bradbury, Gregory Chanan, Trevor Killeen, Zeming Lin, Natalia Gimelshein, Luca Antiga, Alban Desmaison, Andreas Kopf, Edward Yang, Zachary DeVito, Martin Raison, Alykhan Tejani, Sasank Chilamkurthy, Benoit Steiner, Lu Fang, Junjie Bai, and Soumith Chintala. Pytorch: An imperative style, high-performance deep learning library. In *Advances in Neural Information Processing Systems 32*, pages 8024–8035. Curran Associates, Inc., 2019. URL <http://papers.neurips.cc/paper/9015-pytorch-an-imperative-style-high-performance-deep-learning-library.pdf>.
- Victor Sanh, Thomas Wolf, and Alexander M. Rush. Movement pruning: Adaptive sparsity by fine-tuning. *ArXiv*, abs/2005.07683, 2020. URL <https://api.semanticscholar.org/CorpusID:218665313>.
- Mohammad Shoeybi, Mostofa Patwary, Raul Puri, Patrick LeGresley, Jared Casper, and Bryan Catanzaro. Megatron-lm: Training multi-billion parameter language models using model parallelism. *arXiv preprint arXiv:1909.08053*, 2019.
- Rohan Taori, Ishaan Gulrajani, Tianyi Zhang, Yann Dubois, Xuechen Li, Carlos Guestrin, Percy Liang, and Tatsunori B. Hashimoto. Stanford alpaca: An instruction-following llama model. https://github.com/tatsu-lab/stanford_alpaca, 2023.
- Hugo Touvron, Louis Martin, Kevin Stone, Peter Albert, Amjad Almahairi, Yasmine Babaei, Nikolay Bashlykov, Soumya Batra, Prajjwal Bhargava, Shruti Bhosale, et al. Llama 2: Open foundation and fine-tuned chat models. *arXiv preprint arXiv:2307.09288*, 2023a.
- Hugo Touvron, Louis Martin, Kevin Stone, Peter Albert, Amjad Almahairi, Yasmine Babaei, Nikolay Bashlykov, Soumya Batra, Prajjwal Bhargava, Shruti Bhosale, et al. Llama 2: Open foundation and fine-tuned chat models. *arXiv preprint arXiv:2307.09288*, 2023b.
- Jikai Wang, Yi Su, Juntao Li, Qingrong Xia, Zi Ye, Xinyu Duan, Zhefeng Wang, and Min Zhang. Opt-tree: Speculative decoding with adaptive draft tree structure. *Trans. Assoc. Comput. Linguistics*, 13:188–199, 2025. doi: 10.1162/TACL_A_00735. URL https://doi.org/10.1162/tac1_a_00735.
- Yuanxin Wei, Shengyuan Ye, Jiazhi Jiang, Xu Chen, Dan Huang, Jiangsu Du, and Yutong Lu. Communication-efficient model parallelism for distributed in-situ transformer inference. In *2024 Design, Automation & Test in Europe Conference & Exhibition (DATE)*, pages 1–6, 2024. doi: 10.23919/DATE58400.2024.10546617.
- Guangxuan Xiao, Ji Lin, Mickael Seznec, Hao Wu, Julien Demouth, and Song Han. SmoothQuant: Accurate and efficient post-training quantization for large language models. In *Proceedings of the 40th International Conference on Machine Learning*, 2023.
- An Yang, Baosong Yang, Binyuan Hui, Bo Zheng, Bowen Yu, Chang Zhou, Chengpeng Li, Chengyuan Li, Dayiheng Liu, Fei Huang, Guanting Dong, Haoran Wei, Huan Lin, Jialong Tang, Jialin Wang, Jian Yang, Jianhong Tu, Jianwei Zhang, Jianxin Ma, Jin Xu, Jingren Zhou, Jinze Bai, Jinzheng He, Junyang Lin, Kai Dang, Keming Lu, Ke-Yang Chen, Kexin Yang, Mei Li, Min Xue, Na Ni, Pei Zhang, Peng Wang, Ru Peng, Rui Men, Ruize Gao, Runji Lin, Shijie Wang, Shuai Bai, Sinan Tan, Tianhang Zhu, Tianhao Li, Tianyu Liu, Wenbin Ge, Xiaodong Deng, Xiaohuan Zhou, Xingzhang Ren, Xinyu Zhang, Xipin Wei, Xuancheng Ren, Yang Fan, Yang Yao, Yichang Zhang, Yuyang Wan, Yunfei Chu, Zeyu Cui, Zhenru Zhang, and Zhi-Wei Fan. Qwen2 technical report. *ArXiv*, abs/2407.10671, 2024. URL <https://api.semanticscholar.org/CorpusID:271212307>.
- Shengyuan Ye, Jiangsu Du, Liekang Zeng, Wenzhong Ou, Xiaowen Chu, Yutong Lu, and Xu Chen. Galaxy: A resource-efficient collaborative edge ai system for in-situ transformer inference. In *IEEE INFOCOM 2024 - IEEE Conference on Computer Communications*, pages 1001–1010, 2024.
- Shengyuan Ye, Bei Ouyang, Liekang Zeng, Tianyi Qian, Xiaowen Chu, Jian Tang, and Xu Chen. Jupiter: Fast and resource-efficient collaborative inference of generative llms on edge devices. *arXiv preprint arXiv:2504.08242*, 2025.

- Haofei Yin, Mengbai Xiao, Rouzhou Lu, Xiao Zhang, Dongxiao Yu, and Guanghui Zhang. Pipedec: Low-latency pipeline-based inference with dynamic speculative decoding towards large-scale models. *arXiv preprint arXiv:2504.04104*, 2025.
- Mingjin Zhang, Xiaoming Shen, Jiannong Cao, Zeyang Cui, and Shan Jiang. Edgeshard: Efficient llm inference via collaborative edge computing. *IEEE Internet of Things Journal*, pages 1–1, 2024. doi: 10.1109/JIOT.2024.3524255.
- Lianmin Zheng, Wei-Lin Chiang, Ying Sheng, Siyuan Zhuang, Zhanghao Wu, Yonghao Zhuang, Zi Lin, Zhuohan Li, Dacheng Li, Eric P. Xing, Haotong Zhang, Joseph E. Gonzalez, and Ion Stoica. Judging llm-as-a-judge with mt-bench and chatbot arena. *ArXiv*, abs/2306.05685, 2023. URL <https://api.semanticscholar.org/CorpusID:259129398>.

A Extended Experiment Results

A.1 Detailed Experimental Settings

The main experiments were conducted on 5 NVIDIA Jetson Orin Nano units, with the base LLM partitioned across four of these devices. In the main experiments, we set $L = 80$, $d_0 = 6$, and $L_{\max} = 16$ for Gardener and all baseline methods. For Gardener, we further configure $d_{\text{exp}} = 6$ and $L_{\text{exp}} = -1$ where $L_{\text{exp}} = -1$ indicates that all expand tokens are treated as a single input segment. Since expand tokens are pruned prior to transmission, the resulting segments remain small, yielding high efficiency. For PipeDec, we select 16 tokens per layer.

All other experimental settings mirror those of the main experiments.

A.2 Statistical Results

Table 3: **Statistical Results.** This table depicts the outcomes of three independent runs for each model configuration on MT-Bench, evaluated under two sampling settings (temperature = 0 and 1). We selected 10 samples and limit the length of the generated sequences to 128. SD refer to standard deviation. V 7B and L2 7B are short for Vicuna-7B-v1.3 and LLaMA2-Chat 7B, respectively.

Model	Method	Eval 1st		Eval 2nd		Eval 3rd		Mean		SD	
		$\xi \uparrow$	Latency \downarrow	ξ	Latency						
Temperature = 0											
V 7B	Naive PP	5.658	18.320	5.661	18.310	5.659	18.317	5.659	18.316	5.128e-03	5.132e-03
	PipeDec	6.760	14.986	6.770	14.965	6.763	14.979	6.764	14.977	5.132e-03	1.069e-02
	Gardener	7.857	13.091	7.870	13.069	7.892	13.031	7.873	13.064	1.769e-02	3.035e-02
L2 7B	Naive PP	7.022	18.151	7.022	18.149	7.020	18.126	7.021	18.142	1.155e-03	1.389e-02
	PipeDec	7.295	17.218	7.279	17.256	7.291	17.227	7.288	17.234	8.327e-03	1.986e-02
	Gardener	9.396	13.347	9.384	13.363	9.390	13.355	9.390	13.355	6.000e-03	8.000e-03
Temperature = 1											
V 7B	Naive PP	3.936	28.736	3.936	28.734	3.936	28.735	3.936	28.735	0.000e+00	1.000e-03
	PipeDec	6.272	18.541	6.278	18.526	6.277	18.527	6.276	18.531	3.215e-03	8.386e-03
	Gardener	5.408	19.925	5.411	19.913	5.413	19.906	5.411	19.915	2.517e-03	9.609e-03
L2 7B	Naive PP	6.678	18.508	6.684	18.493	6.673	18.522	6.678	18.507	5.508e-03	1.450e-02
	PipeDec	7.216	16.242	7.210	16.256	7.197	16.284	7.208	16.261	9.713e-03	2.139e-02
	Gardener	8.679	14.161	8.700	14.126	8.701	14.125	8.693	14.137	1.242e-02	2.050e-02

The evaluation results exhibit high consistency, as indicated by the extremely small standard deviations. As table 3 depicted, we selected 10 samples from MT-Bench and limited the length of the generated sequences to 128. For all methods across the various models, the standard deviations of both the Average Acceptance Length per Second and the latency are minimal, indicating virtually no fluctuation across the three runs and, consequently, highly stable outcomes.

Empirical results show that Gardener outperforms all other methods. The differences in mean Average Acceptance Length per Second and in latency between Gardener and competing approaches are substantially larger than their standard deviations (SDs), which in turn exceed their standard errors of the mean (SEMs), thereby convincingly demonstrating Gardener’s superiority across diverse evaluation settings.

Under the condition of temperature= 1 on the V 7B model, Naive PP’s Average Acceptance Length per Second is nearly the same across all three runs, resulting in a zero SD of ξ .

B Generation and Parallelism of LLMs

B.1 LLM Inference and Generation

Decoder-only LLM Architecture: Modern LLMs adopt a decoder-only architecture, composed of a token embedding layer followed by multiple stacked transformer decoder layers. Each decoder layer integrates self-attention mechanisms, feed-forward networks (FFNs) and residual connections, enabling LLMs to capture complex contextual dependencies. The final output of the last decoder layer is passed through a classification head to produce probability distributions for the next token. An example is illustrated in the left part of Fig 4.

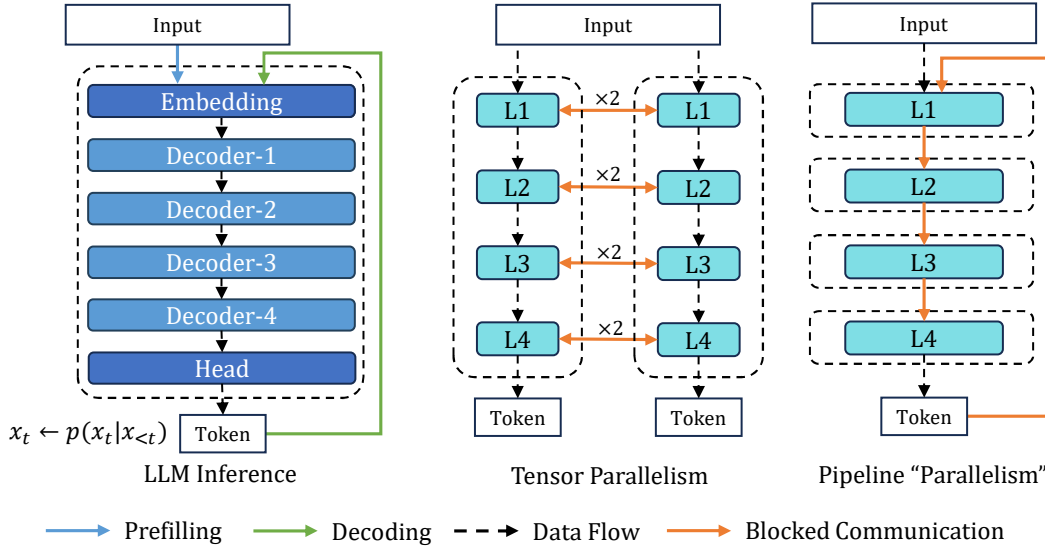


Figure 4: Left: Prefilling and decoding of LLM inference. Right: LLM inference with Tensor Parallelism and Pipeline Parallelism.

Generation Phases of LLMs: The sequence generation of LLMs relies on the key-value caching (KV cache) mechanism, which divides generation process into two phases: **prefilling** and **decoding**. In the **prefilling phase**, the LLM processes the entire input prompt in a single forward pass to generate the probability of the first new token and save the KV cache for all initial input tokens. This phase is characterized by high computational intensity and is typically computation-bottleneck. Then in the **decoding phase**, the LLM autoregressively generates the next new token based on the previous one. Each step involves a low-FLOPs forward propagation and requires frequent access to the KV cache and model parameters, making this phase inherently I/O-bound.

B.2 Parallel Strategies

The growth rate of the model parameter scales far outpaces that of hardware performance improvement, resulting in an increasing demand for distributed LLM deployment. To scale LLM inference efficiently, various parallelism strategies have been proposed.

Data parallelism (DP) distributes distinct inference requests across multiple complete model replicas to enable parallel computation, typically employed to enhance the throughput of training and inference on high-performance computing (HPC) systems, which becomes infeasible in edge scenarios with constrained memory and sparse requests.

Tensor parallelism (TP) decomposes model parameters and splits GEMMs along the hidden dimension within each layer, enabling intra-layer computation parallelism. Although TP reduces per-device memory usage, it requires two All-Reduce operations per layer to synchronize results. In edge systems with low-bandwidth connections, these frequent communications become a major bottleneck. And illustration is shown in the middle part of Fig. 4.

Sequence parallelism (SP) partitions the input along the sequence dimension to enable parallel layer execution. Similar to TP, SP also requires synchronization (e.g., All-Gather) within each layer, but critically, it necessitates a complete model replica on each device. This conflicts with the memory constraints and low-bandwidth nature of typical edge environments, limiting its practicality.

Pipeline parallelism (PP) partitions the model into sequential stages assigned to different devices. By splitting a batch into micro-batches and overlapping inter-stage communication and computation, PP achieve both memory efficient and communication efficiency. However, during the decoding phase, PP faces significant challenges due to the autoregressive nature of token generation, especially in single-request scenarios. As shown in the right part of Fig. 4, in LLM decoding, each new

token depends on the previously generated token, and the forward propagation must be executed sequentially. As a result, when applying pipeline parallelism to decoding, each pipeline stage must frequently wait for the upstream stage to complete its computation before proceeding. This leads to significant idle time and low device utilization, severely limiting the potential speedup of LLM decoding.

In summary, **only the strategies with model partitioning** such as TP and PP can address the memory constraints of edge devices. However, they face key challenges in LLM decoding under edge scenarios. TP suffers from high communication overhead due to frequent synchronization under limited bandwidth, while PP struggles with low concurrency and resource utilization when dealing with sparse inference requests.

C Limitations

Despite the effectiveness and flexibility of our approach, several limitations should be acknowledged. First, our method is based on existing speculative decoding frameworks and is designed to be compatible with most off-the-shelf speculative strategies. However, this also implies that the overall performance of our method is inherently bounded by the quality and efficiency of the underlying speculative decoding baselines.

Second, our pruning mechanism removes redundant draft tokens during verification, which can sometimes result in empty draft segments for certain pipeline stages. This leads to idle computation slots and underutilized resources during the verification of draft token tree. To mitigate this issue, we introduce a tree expansion strategy to fill the draft pool with new candidate tokens, therefore maintaining pipeline activity.

Third, due to the structure of the draft tree and its partitioned step-wise verification process, the number of verification stages cannot be arbitrarily increased. The size of the draft token tree is typically limited and deeper nodes often provide less reliable predictions, making fine-grained splitting of the draft token tree across many stages impractical. To fit large-scale deployment scenarios with abundant devices, combining our approach with other model parallelism techniques such as TP can help control the number of pipeline stages while scaling efficiently.